Structural changes in amorphous GeS_2 at high pressure

M. Vaccari,[1,*] G. Garbarino,[1] G. Aquilanti,[1,2] M.-V. Coulet,[3] A. Trapananti,[4] S. Pascarelli,[1] M. Hanfland,[1] E. Stavrou,[5] and C. Raptis[5]

[1]*European Synchrotron Radiation Facility, 6 rue Jules Horowitz, BP 220, 38043 Grenoble Cedex, France*

[2]*Sincrotrone Trieste, Area Science Park, S.S. 14 km 163.5, Basovizza, 34149 Trieste, Italy*

[3]*IM2NP, UMR CNRS 6242, Université Paul Cezanne, Campus de St Jerôme, 13397 Marseille Cedex 20, France*

[4]*Dipartimento di Fisica, Università di Camerino, 62032 Camerino, Italy*

[5]*Department of Physics, National Technical University of Athens, 15780 Athens, Greece*

(Received 15 June 2009; revised manuscript received 11 October 2009; published 12 January 2010)

High-pressure modifications in glassy GeS_2 have been investigated up to 45 GPa using the diamond anvil cell through x-ray absorption fine structure (XAFS) spectroscopy and x-ray diffraction (XRD). The gradual increase in the Ge-S distance of about 0.1 Å between 15 and 25 GPa evidenced by XAFS is interpreted as a signature of a coordination increase around Ge. The negative shift of the germanium *K* absorption edge position is connected to the progressive metallization of the glass. XRD measurements reveal the amorphous-amorphous nature of the structural transformation. The first sharp diffraction peak loses intensity and shifts toward higher *Q* values in the first few gigapascal, reflecting changes in the intermediate-range order prior to the local coordination increase. The observed changes are reversible after pressure release with strong hysteresis.

DOI: 10.1103/PhysRevB.81.014205 PACS number(s): 61.43.−j, 62.50.−p, 61.05.cj, 61.05.cp

I. INTRODUCTION

The occurrence of amorphous-amorphous transformations (AATs) at high pressure and the concept of polyamorphism are of fundamental interest in glass theory and have drawn much attention in modern condensed-matter physics.[1–3] In recent times, there has been a renewed interest in the nature of high-pressure polyamorphic transitions for a variety of network tetrahedral glasses such as amorphous silicon Si (Ref. 4), germanium Ge (Ref. 5), carbon C (Ref. 6), silica SiO_2 (Ref. 7), germania GeO_2 (Ref. 8), and even carbonia[9] and ice.[10] In contrast to sharp, first-order transitions which take place in crystals, AATs may either be gradual and continuous, as in the case of silica and germania or display a sudden and discontinuous change from a low-density amorphous to an high-density amorphous, as it happens in amorphous ice, silicon, and germanium. The details of coordination increase remain unknown for most AATs and are still matter of intense debate even for basic and well-studied systems.

Numerous experimental and theoretical studies have investigated the fourfold to sixfold change in silica (Ref. 7 and references therein) and germania (Ref. 8 and references therein), but the results obtained by different techniques are controversial. The beginning of the coordination change in amorphous SiO_2 is still discussed in literature[11,12] and high-accuracy quantitative data on Si coordination number through the entire pressure range of interest are not yet available. The possible existence and pressure overlap of two distinct transformations (Ref. 11 and references therein), associated with changes in the intermediate and short-range order, respectively, is still not well clarified. Also concerning amorphous GeO_2 (a-GeO_2), no general agreement was found until recently on the exact pressure range where the AAT takes place.[8,13] Theoretical investigations even do not support the existence of a full octahedral coordination at high pressure and propose a substantial number of pentahedrally coordinated Ge atoms.[14] Moreover, an intermediate glassy form with an average coordination of about five has been claimed[15] but not supported by recent x-ray absorption fine structure (XAFS) results.[8]

High-pressure AATs have been by far less studied in tetrahedral semiconducting chalcogenide glasses, although at least amorphous $GeSe_2$ (a-$GeSe_2$) received some attention: a conversion of edge-sharing (ES) to corner-sharing (CS) tetrahedra and the onset of a coordination increase have been detected below 10 GPa by Raman,[16] high-energy x-ray diffraction (XRD),[17] and acoustic measurements,[18] while a fully completed fourfold to sixfold Ge coordination change has been predicted by molecular-dynamic (MD) simulations at pressures as high as 60 GPa.[19]

At ambient conditions, amorphous chalcogenides have drawn much interest over the past decades because of their optical properties and potential applications in microelectronics and optoelectronics.[20] Besides, amorphous GeS_2 (a-GeS_2) has been for a long time the subject of basic structural investigations.[20–22] Extensive studies on a-GeS_2 were performed concerning: the network dimensionality of the glass,[20,23–26] in comparison with the known crystalline forms of GeS_2; the abundance of ES and CS tetrahedra, and more generally their interpolyhedral linkages which give rise to the intermediate-range order (IRO) of the glass;[27–30] possible evidence of slightly broken chemical order[31–34] as well as of nanoscale phase separations.[35]

With increasing pressure, it has been shown from both *in situ* Raman[20,25] and *in situ* extended XAFS (EXAFS)[36] measurements that a-GeS_2 undergoes a normal densification up to about 10 GPa. This is accompanied by a narrowing of the band gap revealed from optical experiments[23,37]—and by a progressive loss of transparency of the sample.[25] However, to our knowledge, possible AATs in a-GeS_2 at higher pressures have never been experimentally investigated and are therefore the subject of the present study. Only very recently, a

high-density amorphous phase of GeS_2 glass at high pressure has been predicted by *ab initio* calculations.[38]

II. EXPERIMENT

EXAFS and XRD experiments have been performed at the European Synchrotron Radiation Facility (ESRF) at beamlines ID24 (Ref. 39) and ID09A, respectively. High pressure up to 45 GPa was generated by a membrane Le Toullec-type diamond anvil cell (DAC) equipped with conical Boehler-Almax diamonds having a 250-μm-diameter flat culet.

Amorphous GeS_2 was prepared with a direct alloying of the pure elements (Ge 99.9999% and S 99.995%) in the good stoichiometry. The elements were introduced as small pieces in a silica tube and sealed under vacuum. The sample was then slowly heated (0.5 °C/min) up to 1000 °C and the melt was kept at this temperature for 79 h. The temperature was then lowered down to 870 °C for another 24 h (Ref. 35) before quenching in cold water. The sample was kept under vacuum and introduced into a glove box for the further manipulations. A fine powder of sample was loaded in a stainless steel gasket with a hole of 120 μm of diameter and an initial thickness of 40 μm. No pressure transmitting medium was used, thus sacrificing hydrostaticity in favor of the highest possible data quality. The pressure was determined through the ruby fluorescence technique.[40] The ruby sphere was placed close to the border of the cell volume in order to avoid any interaction between the x-ray beam and the ruby, detrimental to the data quality.

Energy-dispersive EXAFS data were recorded at the Ge *K* edge (11.1 keV) using a two-dimensional CCD detector (FReLoN camera).[41] The beam was focused horizontally by a curved polychromator Si 111 crystal in a Bragg geometry and vertically by two bent Rh and Pd mirrors with grazing incidence of 3 and 4 mrad, respectively. The x-ray beam spot size on the sample was about 20×20 μm^2. A pixel-to-energy calibration was conducted by measuring an amorphous Ge foil at ambient conditions and comparing it with a reference spectrum taken in the standard energy-scanning x-ray absorption spectroscopy beamline BM29 (Ref. 42) at ESRF.

Angle-dispersive powder XRD patterns were recorded using a MAR555 image plate detector placed at about 34 cm from the sample. The wavelength was tuned to 0.4148 Å through a Si 111 monochromator. The beam was focused to 20×20 μm^2. The typical exposure time was about 5 s and during exposure the cell was rotated by $\pm5°$ to improve powder averaging.

III. RESULTS

A. EXAFS

X-ray absorption data have been analyzed through established procedures[8] by using the ATHENA and ARTEMIS programs of the IFEFFIT package.[43,44] The Bragg diffraction peaks arising from the diamond anvils were removed as much as possible from the energy range of interest by selecting the proper orientation of the DAC. Nonetheless, they limited the exploitable energy range of the spectra to about 250 eV after the edge (Fig. 1).

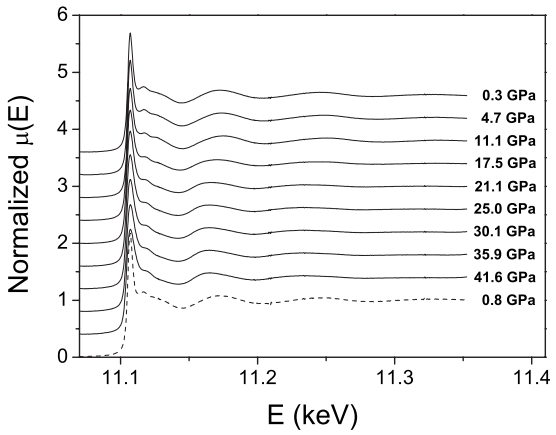

FIG. 1. Normalized absorption spectra at the Ge *K* edge of amorphous GeS_2 at selected increasing pressures from top to bottom (continuous lines) and of the sample recovered at nearly ambient pressure (dashed line).

The EXAFS signal was obtained as $\chi(k)=(\mu-\mu_0)/\mu_0$, where μ is the experimental absorption coefficient and μ_0 is a smooth spline representing the embedded-atom absorption background. The energy to wave-vector conversion $k=(2m/\hbar^2)[E-E_b]$ was performed by setting the edge energy E_b to the zero crossing of the second derivative for each pressure value. The Ge *K* absorption edge position is found to shift toward lower energies by about −1.2 eV in the first 20 GPa; this change is fully reversible but with strong hysteresis (Fig. 2). The overall edge shift becomes clear also by visual inspection by comparing the near-edge absorption spectra at low and high pressure, as shown in the inset of Fig. 2. This negative-edge shift is connected to the pressure-induced metallization of a-GeS_2, already known in the literature (see Sec. IV).

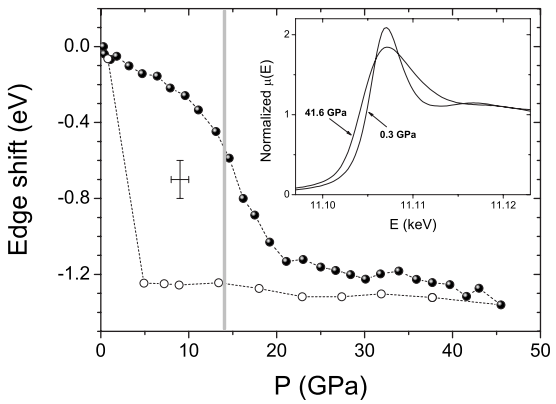

FIG. 2. Energy variation in the Ge *K* absorption edge position as a function of increasing and decreasing pressure (filled and open circles, respectively). The estimated error bar is shown separately in the graph. The dashed line is only a guide for the eyes. The gray vertical line roughly marks the beginning of the coordination increase as found from EXAFS analysis (see Fig. 4). In the inset, the near-edge absorption spectra at low and high pressure are compared. The overall edge shift is clear.

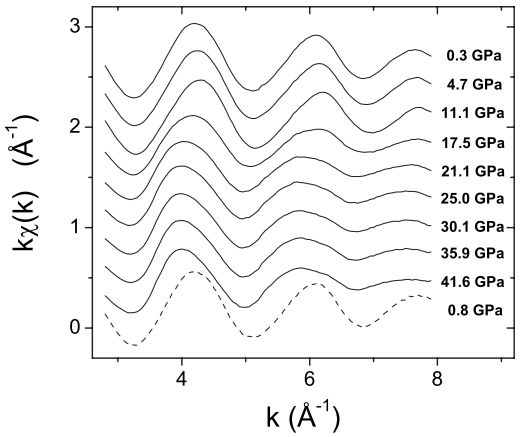

FIG. 3. Extracted $k\chi(k)$ EXAFS signals of amorphous GeS_2 at selected increasing pressures from top to bottom (continuous lines) and of the sample recovered at nearly ambient pressure (dashed line). These data have been rebinned to a 0.05 Å^{-1} grid.

The extracted EXAFS data (Fig. 3) have been interpreted in terms of a single Ge-S shell, by using theoretical amplitudes and phases calculated by FEFF6. The $\chi(k)$ signals were fitted in k space with a fitting interval of 2.5–7.5 Å^{-1}, corresponding to the peak between 0.8 and 2.5 Å in the Fourier-transformed R space. The amplitude reduction factor S_0^2 and the energy mismatch e_0 between experimental and theoretical scales were set to about 1.0 and 5.8 eV, respectively. The very short k range of the data (Fig. 3) limited the accuracy of interatomic distances to about 0.02 Å and prevented to get accurate information concerning the coordination number.

The obtained evolution for the Ge-S bond length is shown in Fig. 4. Below about 13 GPa there is a bond compression of about 0.03 Å, while between 15 and 25 GPa the average Ge-S distance undergoes a gradual elongation of about 0.1 Å. This is interpreted as the signature of a structural transformation which implies a coordination increase. The σ^2 parameter increases of about 0.01 Å^2 at the transformation, due to the higher degree of structural disorder of bond

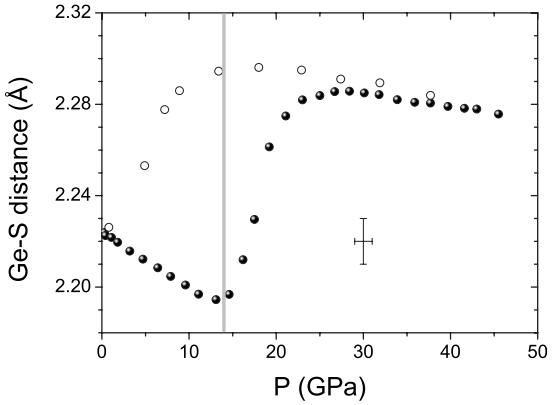

FIG. 4. Evolution of the Ge-S average distance as a function of increasing and decreasing pressure (filled and open circles, respectively). The typical error bar is shown separately in the graph. The gray vertical line roughly marks the beginning of the coordination increase.

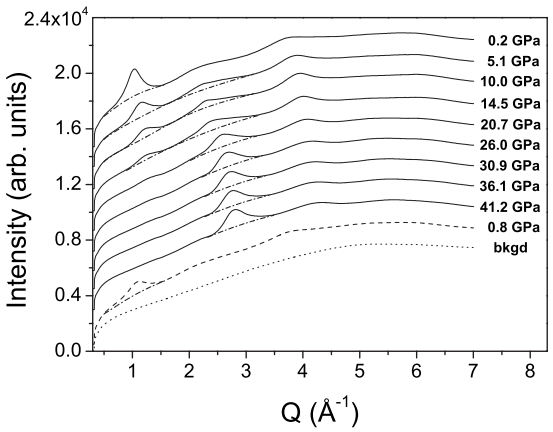

FIG. 5. X-ray diffraction patterns of amorphous GeS_2 at selected increasing pressures from top to bottom (continuous lines), of the sample recovered at nearly ambient pressure (dashed line) and of the measured empty-cell background (dotted line). The dash-dotted lines show the baselines subtracted to estimate the Q position of the FSDP and PP in Fig. 6.

lengths in the high-pressure glass. The exact pressure range of transition and its width should be taken with caution, since they could be influenced by the nonhydrostatic conditions which lead to unavoidable pressure gradients in the DAC. After 25 GPa the Ge-S distance slightly reduces up to the maximum pressure reached, suggesting that a compression of higher coordination polyhedra is taking place and that the glass in well converted to its high-pressure modification. This structural change observed in a-GeS_2 is reversible, although with large hysteresis (Fig. 4): when pressure is released, the Ge-S distance first slightly increases, then below 10 GPa suddenly decreases down to the original value of 2.22(1) Å.

B. XRD

Two-dimensional image plate data were integrated with FIT2D (Ref. 45) to produce intensity patterns as a function of the wave vector Q. Single-diffraction spots from the diamond anvils were manually masked and excluded from the integration. The DAC angular opening limited the good Q range of the diffractograms to about 7 Å^{-1} (Fig. 5). The XRD data show that the structural transformation in a-GeS_2 evidenced by EXAFS has an amorphous-amorphous nature and that no crystallization takes place.

Diffraction patterns are strongly influenced by the background scattering contributions from the diamond anvils and the air. This background (dotted line in Fig. 5) has been evaluated by performing an empty-cell measurement, i.e., with the DAC mounted in the beam with the same orientation but with no sample inside. Given the extremely limited value of Q_{max}, as well as the lack of knowledge of the density for the high-pressure amorphous modification and the impossibility to measure the incident-beam intensity, we did not attempt any background subtraction and data normalization. Only the position of the first sharp diffraction peak (FSDP) and the following principal peak (PP) has been determined from the XRD patterns by fitting them with a

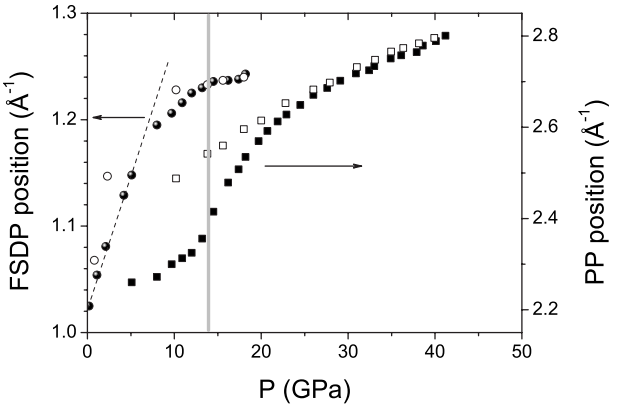

FIG. 6. Q position of the FSDP (circles, left-hand axis) and PP (squares, right-hand axis) as a function of increasing and decreasing pressure (filled and open symbols, respectively). The dashed line emphasizes the linear behavior of the FSDP in the first few gigapascal. The gray vertical line roughly marks the beginning of the coordination increase.

Gaussian curve after subtraction of a reasonable baseline (dash-dotted lines in Fig. 5). At ambient conditions, the FSDP is found at $Q=1.02$ Å^{-1} and the PP at $Q\sim 2.2$ Å^{-1}, in agreement with the values found from neutron diffraction.[33] The FSDP exhibits a nearly linear shift with pressure up to about 7 GPa (Fig. 6) and almost disappears above about 20 GPa; the PP gains intensity after a few gigapascal and shifts upwards by about 0.6 Å^{-1} over the entire pressure range of the study (Figs. 5 and 6).

IV. DISCUSSION

The Ge-S bond compression found at the lowest pressures (Fig. 4) is in agreement with previous EXAFS findings[36] and consistent with relevant Raman data.[25] Also for a-Ge a bond shortening was detected in the low-pressure region,[5] while for a-GeO_2 the absence of a decrease in the average Ge-O distance before any coordination change has been recently pointed out.[8]

The gradual elongation of the average Ge-S distance in the 15–25 GPa pressure range is interpreted as the conversion from a tetrahedral glass to a mainly octahedrally coordinated amorphous state, in close analogy with the same phenomenon measured in germania[13] at lower pressures. The Ge coordination number, qualitatively equal to four in the low-pressure range, becomes roughly compatible with six well after the transition. However, given the important experimental uncertainty on the coordination number (± 2 at high pressure) and the fact that only average quantities are probed, we cannot exclude the possible coexistence of fourfold, fivefold, and sixfold coordinated Ge atoms over all the pressure range and with pressure-dependent proportions, as suggested by *ab initio* MD.[38] In more detail, Durandurdu[38] proposed a very consistent percentage of fivefold coordinated Ge atoms even at 60 GPa, thus not supporting the existence of a fully octahedral state in the high-pressure glass. As a matter of fact, existing simulations predict a significant fraction of five-coordinated Ge atoms also in the case of a-GeO_2 (see, for example, Ref. 14), but the proposed average distance does not reproduce the available experimental results (see discussion in Ref. 8). Moreover, in a-GeO_2 the fourfold-to-sixfold nature of the transition seems well established, at least by comparison with the analogous behavior in crystalline quartzlike GeO_2.[13]

The full reversibility of the structural change observed in a-GeS_2 (Fig. 4) prevents any meaningful investigation on recovered samples: the higher coordination state cannot be recovered at ambient conditions and therefore the AAT must be studied *in situ*. With pressure release, the glass tries to maintain as long as possible the more compacted high-density modification: this originates a large hysteresis (Fig. 4), in analogy with the overall behavior found in a-GeO_2 (see Ref. 13). One might also wonder if possible Ge-Ge homopolar bonds play a role in the observed transition. At ambient conditions, Ge-Ge bonds are present in a-GeS_2 only in minimal quantities (probably 1% or less).[33–35] In a ternary Ge-As-S glass, the changes induced by pressure at 2 GPa and explained by the formation of Ge-GeS_3 ethanelike units have been shown to be irreversible by Raman spectroscopy.[46] Therefore, the reversibility itself of the transition observed in this study suggests that it is not connected to the possible formation of Ge-Ge bonds at high pressure. This is consistent with the conclusions of Durandurdu[38] for a-GeS_2: his recent *ab initio* calculations are not significantly affected by possible Ge-Ge homopolar bonds.

The pressure-induced semiconducting-metallic change evidenced in a-GeS_2 from the negative shift of the Ge K absorption edge (Fig. 2) is consistent with the band-gap closure measured by optical experiments[23,37] limited to lower pressures. Also for amorphous germanium[5] a backward shift of the Ge K absorption edge of about 1 eV was measured by XAFS and connected to the metallization of the glass. However, contrary to recent *ab initio* molecular dynamics,[38] we point out that the band-gap closure is not necessarily associated to (or induced by) the structural conversion: by comparing Figs. 2 and 4, it is clear that the process of metallization is already present when the Ge-S bond compression is still active and that half of the whole edge shift already took place at the onset of the coordination increase. In the case of a-GeO_2, a Ge K absorption edge shift toward higher energies was reported[8] in the same pressure range of the coordination increase.

With increasing pressure, the FSDP progressively loses intensity (Fig. 5) and shifts toward higher Q values (Fig. 6), in qualitative agreement with previous diffraction measurements[37] limited to 7 GPa. These modifications of the FSDP are not directly correlated with the short-range order but rather reflect changes in the IRO in the tetrahedral network upon compression, which occur before the local Ge coordination increase evidenced by EXAFS. The overall evolution of the FSDP position resembles what happens for a-GeO_2 (Ref. 47). Also in a-$GeSe_2$ a positive shift of both the FSDP and PP, as well as dramatic changes in their intensities, were found by high-energy diffraction up to 9.3 GPa.[17] In network AX_2 glasses the PP has been associated by Salmon *et al.*[48] to an extended range order. In the framework of the density-dependent structural transitions that occur in tetrahedral network glasses, the inter-relation and competition be-

tween ordering on the intermediate and extended length scales is still matter of investigation.[49]

The present evidence of a structural AAT in a-GeS_2 in the 15–25 GPa pressure range can be compared with previous experimental findings on a-GeO_2, for which the analogous coordination increase roughly takes place between 5 and 15 GPa,[8,50] as well as with simulations on a-$GeSe_2$ which predict that pressures as high as 60 GPa would be necessary to produce a complete fourfold to sixfold Ge coordination change.[19] Therefore, we might argue that within the family of tetrahedral amorphous GeX_2 (X=O,S,Se) systems the pressure range of transition at which the fourfold to sixfold change takes place increases with X atomic weight. The fact that usually "elements behave at high pressure like the elements below them in the periodic table at lower pressures" (Refs. 51 and 52) has been currently cited in the past, for example, in studies of silicates: researchers preferred to explore the analogous germanates, for which similar phase transitions were observed at more easily accessible pressures.[13] Therefore, the result of a higher pressure range of transition in a-GeS_2 with respect to a-GeO_2, as well as the conjecture that the application of even higher pressure would be needed to produce an analogous change in a-$GeSe_2$ can be regarded as counterintuitive.

Amorphous GeX_2 (X=O,S,Se) materials are characterized by a different degree of Ge-X bond covalency, which obviously increases with increasing X atomic weight: the Pauling bond ionicity is more than 40% for Ge-O but is only around 10% for Ge-S and even smaller for Ge-Se bonds. For many elements, including the ones of interest in this work, the Pauling electronegativity scale used to estimate bond ionicity has been roughly confirmed by more recent first-principles calculations.[53] Although both a-GeO_2 and a-GeS_2 are made up of tetrahedral building blocks, the two systems are characterized by a different kind of IRO at ambient conditions: while the intertetrahedral angle Ge-$\hat{O}$-Ge in a-GeO_2 is around 132° due to CS GeO_4 tetrahedra, the intertetrahedral angle Ge-$\hat{S}$-Ge in a-GeS_2 includes a first contribution caused by ES GeS_4 tetrahedra and centered around 80° and a second contribution due to CS tetrahedra and located at about 100°.[30,38] Therefore the detailed mechanism of response to applied pressure is actually expected to differ in detail between a-GeS_2 and a-GeO_2, in view of their very different bond ionicity and polyhedral connectivity. The occurrence of two densification processes, namely, a conversion from edge-to-corner-shared tetrahedra and the onset of a coordination increase, was suggested in the case of a-$GeSe_2$ below 10 GPa.[16–18] Further theoretical and/or experimental studies are necessary to shed light into the structural changes occurring at intermediate length scale in a-GeS_2. Since the present manuscript was submitted, a new structural investigation of glassy GeS_2 was performed by using *in situ* neutron and x-ray diffraction up to 5 GPa (Ref. 54): according to these authors, the changes at intermediate length scale are consistent with a replacement of ES by CS tetrahedra and/or a reduction in the intertetrahedral angle Ge-$\hat{S}$-Ge between CS tetrahedra.

V. CONCLUSIONS

In this work we have performed an *in situ* high-pressure EXAFS and diffraction investigation of amorphous GeS_2 up to 45 GPa. The main finding of this study is the gradual elongation of the Ge-S distance over the pressure range 15–25 GPa, which is attributed to an increase in the average Ge-S coordination number and which therefore implies the existence of two structurally distinct amorphous modifications of a-GeS_2 in different pressure regions. The Ge K absorption edge position is found to shift toward lower energies with increasing pressure, thus confirming the known pressure-induced metallization in a-GeS_2 which precedes the onset of structural transition. The observed changes are reversible after pressure release with strong hysteresis. The decrease in intensity and the positive Q shift of the FSDP in the first few gigapascal evidence changes in the intermediate-range order, which take place before the local coordination increase. While this work provides experimental evidence of high-pressure polyamorphism, the physics underlying AATs is still far from being completely clarified and its full understanding requires further investigations.

ACKNOWLEDGMENTS

The European Synchrotron Radiation Facility (ESRF) is acknowledged for provision of beam-time through the project HD-361. The authors are grateful to P. Boolchand, W. Crichton, and A. Polian for helpful advice, to K. Woodhead for experimental assistance, and to J. Jacobs, P. van der Linden, H. Mueller, F. Perrin, S. Pasternak, and M. C. Dominguez for technical help.

*vaccari@esrf.fr

[1] P. H. Poole, T. Grande, F. Sciortino, H. E. Stanley, and C. A. Angell, Comput. Mater. Sci. **4**, 373 (1995).
[2] V. V. Brazhkin and A. G. Lyapin, J. Phys.: Condens. Matter **15**, 6059 (2003).
[3] M. C. Wilding, M. Wilson, and P. F. McMillan, Chem. Soc. Rev. **35**, 964 (2006).
[4] D. Daisenberger, M. Wilson, P. F. McMillan, R. Quesada Cabrera, M. C. Wilding, and D. Machon, Phys. Rev. B **75**, 224118 (2007).
[5] A. Di Cicco, A. Congeduti, F. Coppari, J. C. Chervin, F. Baudelet, and A. Polian, Phys. Rev. B **78**, 033309 (2008).
[6] Y. X. Wei, R. J. Wang, and W. H. Wang, Phys. Rev. B **72**, 012203 (2005).
[7] T. Sato and N. Funamori, Phys. Rev. Lett. **101**, 255502 (2008).
[8] M. Vaccari, G. Aquilanti, S. Pascarelli, and O. Mathon, J. Phys.: Condens. Matter **21**, 145403 (2009).
[9] M. Santoro, F. A. Gorelli, R. Bini, G. Ruocco, S. Scandolo, and W. A. Crichton, Nature (London) **441**, 857 (2006).
[10] C. A. Angell, Annu. Rev. Phys. Chem. **55**, 559 (2004).

[11] V. V. Brazhkin, Phys. Rev. Lett. **102**, 209603 (2009).
[12] N. Funamori and T. Sato, Phys. Rev. Lett. **102**, 209604 (2009).
[13] J. P. Itie, A. Polian, G. Calas, J. Petiau, A. Fontaine, and H. Tolentino, Phys. Rev. Lett. **63**, 398 (1989).
[14] K. V. Shanavas, N. Garg, and S. M. Sharma, Phys. Rev. B **73**, 094120 (2006).
[15] M. Guthrie, C. A. Tulk, C. J. Benmore, J. Xu, J. L. Yarger, D. D. Klug, J. S. Tse, H.-k. Mao, and R. J. Hemley, Phys. Rev. Lett. **93**, 115502 (2004).
[16] F. Wang, S. Mamedov, P. Boolchand, B. Goodman, and M. Chandrasekhar, Phys. Rev. B **71**, 174201 (2005).
[17] Q. Mei, C. J. Benmore, R. T. Hart, E. Bychkov, P. S. Salmon, C. D. Martin, F. M. Michel, S. M. Antao, P. J. Chupas, P. L. Lee, S. D. Shastri, J. B. Parise, K. Leinenweber, S. Amin, and J. L. Yarger, Phys. Rev. B **74**, 014203 (2006).
[18] S. M. Antao, C. J. Benmore, B. Li, L. Wang, E. Bychkov, and J. B. Parise, Phys. Rev. Lett. **100**, 115501 (2008).
[19] M. Durandurdu and D. A. Drabold, Phys. Rev. B **65**, 104208 (2002).
[20] I. P. Kotsalas and C. Raptis, J. Optoelectron. Adv. Mater. **3**, 675 (2001).
[21] S. C. Rowland, S. Narasimhan, and A. Bienenstock, J. Appl. Phys. **43**, 2741 (1972).
[22] G. Lucovsky, F. L. Galeener, R. C. Keezer, R. H. Geils, and H. A. Six, Phys. Rev. B **10**, 5134 (1974).
[23] B. A. Weinstein, R. Zallen, M. L. Slade, and J. C. Mikkelsen, Jr., Phys. Rev. B **25**, 781 (1982).
[24] Z. Černošek, E. Černošková, and L. Beneš, J. Mol. Struct. **435**, 193 (1997).
[25] A. Perakis, I. P. Kotsalas, E. A. Pavlatou, and C. Raptis, Phys. Status Solidi B **211**, 421 (1999).
[26] I. P. Kotsalas and C. Raptis, Phys. Rev. B **64**, 125210 (2001).
[27] A. Feltz, M. Phole, H. Steil, and G. Herms, J. Non-Cryst. Solids **69**, 271 (1985).
[28] P. Armand, A. Ibanez, H. Dexpert, and E. Philippot, J. Non-Cryst. Solids **139**, 137 (1992).
[29] X. Zhao, H. Higuchi, and Y. Kawamoto, Phys. Chem. Glasses **39**, 98 (1998).
[30] S. Blaineau, P. Jund, and D. A. Drabold, Phys. Rev. B **67**, 094204 (2003).
[31] W. J. Bresser, P. Boolchand, P. Suranyi, and J. P. de Neufville, Phys. Rev. Lett. **46**, 1689 (1981).
[32] P. Boolchand, J. Grothaus, M. Tenhover, M. A. Hazle, and R. K. Grasselli, Phys. Rev. B **33**, 5421 (1986).
[33] I. Petri and P. S. Salmon, J. Non-Cryst. Solids **293-295**, 169 (2001).
[34] S. Blaineau and P. Jund, Phys. Rev. B **69**, 064201 (2004).
[35] L. Cai and P. Boolchand, Philos. Mag. B **82**, 1649 (2002).
[36] K. Miyauchi, J. Qiu, M. Shojiya, Y. Kawamoto, N. Kitamura, K. Fukumi, Y. Katayama, and Y. Nishihata, Solid State Commun. **124**, 189 (2002).
[37] K. Tanaka, J. Non-Cryst. Solids **90**, 363 (1987).
[38] M. Durandurdu, Phys. Rev. B **79**, 205202 (2009).
[39] S. Pascarelli, O. Mathon, M. Muñoz, T. Mairs, and J. Susini, J. Synchrotron Radiat. **13**, 351 (2006).
[40] R. A. Forman, G. J. Piermarini, J. D. Barnett, and S. Block, Science **176**, 284 (1972).
[41] J.-C. Labiche, O. Mathon, S. Pascarelli, M. Newton, G. Guilera, C. Curfs, G. Vaughan, A. Homs, and D. F. Carreiras, Rev. Sci. Instrum. **78**, 091301 (2007).
[42] A. Filipponi, M. Borowski, D. T. Bowron, S. Ansell, A. Di Cicco, S. De Panfilis, and J. P. Itié, Rev. Sci. Instrum. **71**, 2422 (2000).
[43] M. Newville, J. Synchrotron Radiat. **8**, 322 (2001).
[44] B. Ravel and M. Newville, J. Synchrotron Radiat. **12**, 537 (2005).
[45] A. P. Hammersley, S. O. Svensson, A. Thompson, H. Graafsma, Å. Kvick, and J. P. Moy, Rev. Sci. Instrum. **66**, 2729 (1995).
[46] Y. C. Boulmetis, E. Stavrou, and C. Raptis, Phys. Status Solidi B **244**, 256 (2007).
[47] X. Hong, G. Shen, V. B. Prakapenka, M. Newville, M. L. Rivers, and S. R. Sutton, Phys. Rev. B **75**, 104201 (2007).
[48] P. S. Salmon, A. C. Barnes, R. A. Martin, and G. J. Cuello, Phys. Rev. Lett. **96**, 235502 (2006).
[49] P. S. Salmon, J. Phys.: Condens. Matter **19**, 455208 (2007).
[50] X. Hong, M. Newville, V. B. Prakapenka, M. L. Rivers, and S. R. Sutton, Rev. Sci. Instrum. **80**, 073908 (2009).
[51] W. Grochala, R. Hoffmann, J. Feng, and N. W. Ashcroft, Angew. Chem., Int. Ed. **46**, 3620 (2007).
[52] C. T. Prewitt and R. T. Downs, Rev. Mineral. **37**, 283 (1998).
[53] A. García and M. L. Cohen, Phys. Rev. B **47**, 4221 (1993).
[54] A. Zeidler, J. W. E. Drewitt, P. S. Salmon, A. C. Barnes, W. A. Crichton, S. Klotz, H. E. Fischer, C. J. Benmore, S. Ramos, and A. C. Hannon, J. Phys.: Condens. Matter **21**, 474217 (2009).